Preparation and Photo-Fenton Activity of Nano Perovskite Oxides of $CeBa_{1-x}Fe_xO_{3-\delta}$ (X=0, 0.5, 1) by Sol-Gel Method

A. ANANTHARAMAN [1], A. PAUL RAJ[2] AND M. GEORGE[1*]

[1, 1*]Department of Chemistry, Stella Maris College, Chennai, Tamilnadu, India
[2]Department of Physics, Loyola College, Chennai, Tamilnadu, India
Corresponding Author email: maryge@gmail.com

Abstract

Rare-earth nano sized perovskite ferrites are the most considerable class of materials due to their exceptional structural, optical and magnetic properties. $CeBa_{1-x}Fe_xO_{3-\delta}$ nano mixed perovskite oxides with varying mole ratios (x=0, 0.5 and 1) were synthesized via sol-gel method. The synthesized nanomaterials were characterized using FT-IR, PXRD, HR-TEM, UV-Visible and VSM techniques. XRD analysis showed that the $CeBa_{0.5}Fe_{0.5}O_{3-\delta}$ oxides were nanocrystalline with orthorhombic structure. The optical studies reveal that $CeBa_{1-x}Fe_xO_{3-\delta}$ oxides are semiconductors with highest band gap value observed in $CeBa_{0.5}Fe_{0.5}O_{3-\delta}$ than pure oxides. The magnetic analysis from VSM measurements showed that $CeBa_{0.5}Fe_{0.5}O_{3-\delta}$ mixed metal oxide nanoparticles were weakly ferromagnetic and exhibit as a soft ferrite. The photocatalytic activities of $CeBa_{1-x}Fe_xO_{3-\delta}$ nanoparticles were evaluated by the photodegradation of methylene blue UV-Visible light irradiation. The photocatalytic results suggest that the degradation efficiency was 99% for $CeBa_{0.5}Fe_{0.5}O_{3-\delta}$ nano perovskite mixed metal oxide and the reaction followed pseudo-first order kinetics. Oxygen vacancies, substitution of divalent metal cation and the strong absorption in visible light increased the photocatalytic activity of cerium barium ferrite.

Keywords: Nano Perovskite oxide; sol-gel; dye degradation; photo fenton activity

Introduction

Perovskite type mixed metal oxides with the general formula ABO_3 in which A is a rare earth or alkali earth ion and B is 3d, 4d or 5d transition metal ion are multifunctional materials. Further, substitution in both A and B sites can change the composition and symmetry of the oxides and create cations or oxygen vacancies, which have a vital influence on the band structures and the photocatalytic behavior of these materials [1]. Magnetic composite systems such as TiO_2/iron oxide, anatase TiO_2 nanoparticle coating on magnetic particles including barium ferrite, Fe_3O_4, nickel ferrite are being reported in literature [2]. Due to the non-stoichiometric nature of the cation or anion, the distortion of the cation configuration and the electronic structure arising from mixed-valence perovskite and perovskite-related materials exhibit versatile physical and chemical properties such as colossal magnetoresistance, ferroelectricity, superconductivity, charge ordering, spin dependent transport, high thermo power and the interplay of structural, magnetic and transport properties and intriguing properties [3,4]from both the theoretical and the application point of view have attracted considerable research interest in materials chemistry.

Rare earth ferrites [5] has attracted great attention among researchers due to their useful properties in various promising applications ranging from solid oxide fuel cells[6], dye sensitized solar cells[7], sensors[8], environmental catalysts[9] to magnetic materials[10]. The mixed valence states of Fe^{2+}/Fe^{3+} existing between the 3d iron ions in $RFeO_3$ ceramics is due to the anion deficiency, making

them prominent electric and magnetic materials[11]. An electron hopping process occurs in $RFeO_3$-based perovskites between the $Fe^{3+}$and Fe^{2+}ions[12].Among the various oxide based semiconductor photocatalysts, TiO_2 has received intensive attention due to the advantages of low-cost, high activity, photochemical stability and environmental friendliness. However, TiO_2 can only absorb the ultraviolet (UV) light occupying a small fraction of <6% of the solar energy due to its large band gap which confines its practical applications. Many efforts have been made to study the optical response of TiO_2 under visible-light region including nonmetal (e.g. N, C, F, S) or transition metal doping (e.g. Cr, Cu, Fe), organic dyes sensitizing etc. [13-14]. But, the photocatalytic activity was found to be still low, and there were problems in achieving stability or applicability.

Photocatalysis has quite a lot of promising applications in the environmental field. A wide range of materials systems have been developed over the past two decades as the number of applications based on photocatalysis such as degradation of volatile organic compounds (VOC) for water treatment [15], germicide and antimicrobial action [16], decoloration of industrial dyes[17], nitrogen fixation in agriculture[18], and removal of NO_x/So_x air pollutants[19–20]. These applications have led to the development of variety of materials systems which are appropriate for specific applications. Rare earth and bismuth-based double perovskites with general formula Ba_2RBiO_6 where (R = La, Ce, Pr, Nd, Sm, Eu, Gd, Dy) were prepared and their photocatalytic activity was studied for methylene blue degradation [21].The band gap value of $LaCoO_3$ was found to be 2.7 eV and the oxygen deficient $LaCoO_{3-\delta}$ has been studied for methyl orange degradation (>400 nm)[22].

The environmental issues associated with organic dyes from textile and dying, paper and other industries remain to be the main concern. Therefore, more effort has been devoted in developing heterogeneous nanocatalysts which would serve as a popular material to study the photodegradation of dyes from the environment. Methylene Blue (MB) is one among the dyes used in printing, paper, textile and dying, pharmaceutical and food industries [23, 24] with the chemical formula $C_{16}H_{18}N_3SCl$. The structure of methylene blue dye is given in Figure.1 and the maximum absorption peak recorded in the UV spectrum is 665nm.Investigation of the structural, optical and magnetic properties and the photocatalytic potential of the $CeBa_{1-x}Fe_xO_{3-\delta}$ nanoparticles are the main objectives of the present study.

Experimental Work

All the chemicals purchased for the synthesis of cerium barium ferrite nanoparticles were used as such without any further purification. Analytical grade $CeN_3O_9.6H_2O$ (SDFCL), barium nitrate (Fischer Scientific), Iron nitrate (Fischer Scientific), $C_6H_8O_7.H_2O$ (Fischer Scientific), ethylene glycol(Fischer Scientific) and deionized water were used as precursors for the synthesis of $CeBa_{1-x}Fe_xO_{3-\delta}$ (x=0, 0.5 and 1) mixed metal oxides. Methylene Blue (Nice chemicals) and hydrogen peroxide ((Fischer Scientific) was used for dye degradation studies.

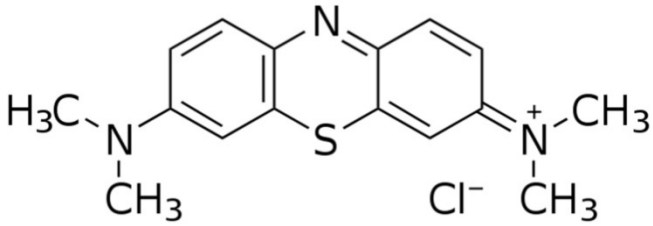

Figure.1. Structure of Methylene Blue dye

Nano perovskite oxides $CeBa_{1-x}Fe_xO_{3-\delta}$ (x=0, 0.5and 1) with varying mole ratios were synthesized using citric acid sol-gel method. The required precursors containing nitrates in appropriate mole ratios were dissolved in deionized water to form clear homogeneous solution. The mixture containing citric acid and ethylene glycol were heated and stirred at 100°C.Then, the above solution was heated and stirred in a magnetic stirrer at 150°C and kept for gellation at 300°C for 3 h in air oven. The obtained gel was sintered in muffle furnace at 800°C for 8 hours and the resulting powder was used for further characterization studies. The corresponding chemical reactions for the synthesized materials are as follows

$$Ce(NO_3)_2.6H_2O + Ba(NO_3)_2 + 3C_6H_8O_7 + C_6H_6O_2 \xrightarrow{800^\circ C / 8\ hrs} CeBaO_3$$

$$Ce(NO_3)_2.6H_2O + Ba(NO_3)_2 + Fe(NO_3)_3.9H_2O + 3C_6H_8O_7 + C_6H_6O_2 \xrightarrow{800^\circ C / 8\ hrs} CeBa_{1-x}Fe_xO_{3-\delta}$$

$$Ce(NO_3)_2.6H_2O + + Fe(NO_3)_3.9H_2O + 3C_6H_8O_7 + C_6H_6O_2 \xrightarrow{800^\circ C / 8\ hrs} CeFeO_3$$

Photo degradation of Methylene Blue using $CeBa_{1-x}Fe_xO_{3-\delta}$ (x=0, 0.5 and 1) perovskite nano mixed metal oxides

The photo degradation experiment was carried out in 100mL quartz tubes containing 25ppm methylene blue solution and 0.1g of catalyst using a UV multi - lamp photoreactor [Heber HML – COMPACT- LP-MP88]. The photoreactor was fitted with six numbers of 8Wmercury vapor lamps (Sankyo denki, Japan) emitting wavelengths with maximum spectral intensity at 365 nm and the reaction chamber was made of highly polished anodized aluminum with built-in cooling fans. The experiment was performed by aerating continuously, which served as the oxygen source for the thorough mixing of the solution. Preliminary reactions were done to monitor the variations in dark and under UV-lamp irradiation with hydrogen peroxide. The degradation studies were performed for 180 minutes. The different aliquots were collected and centrifuged to remove the particles for every 30 minutes and the absorbance was measured with UV-Visible spectrophotometer. The degradation efficiency of the nano photocatalysts was calculated using the following equation

$$\%\deg radation = \frac{Co - Ct}{C0} \times 100 \quad (1)$$

Where C_o and C_t represent the initial concentration and concentration at time t respectively.

Determination of oxygen non-stoichiometry

The oxygen non-stoichiometry δ of pure and mixed metal oxide was determined by Bunsen-Rupp method. In this method, the samples on digestion with concentrated hydrochloric acid leads to reduction of ceriumions. Thus, the evolved chlorine was studied by iodometric titration [25].

Results and Discussion

Powder X-ray diffraction studies

The XRD patterns of $CeBaO_3$ (CBFO-1), $CeBa_{0.5}Fe_{0.5}O_{3-\delta}$ (CBFO-2)and $CeFeO_3$ (CBFO-3) oxides, prepared by sol-gel method and sintered at 800°C for 8h are shown in Figure.2. It can be seen that the diffraction pattern were in good agreement with standard pattern of perovskite oxide. The unit cell

corresponding to the synthesized mixed oxides has undergone distortion from its basic cubic structure. The reason for modification in crystal system from cubic to orthorhombic system may be because of difference in type and extent of distortion of Fe_2O_3 octahedra along the three basic crystallographic axis of the cubic perovskite cell [26].The average crystallite size of the synthesized particles were calculated using the Debye-Scherrer's formula $D = \frac{0.89\lambda}{\beta \cos\theta}$ (2)

Where D is the average crystallite size, λ is the wavelength emitted from X-rays, β is Full Width Half Maximum (FWHM) and θ represents the corresponding Bragg's angle. The average crystallite size of pure $CeBaO_3$ (CBFO-1) and $CeFeO_3$ (CBFO-3) oxides were found to be 36nm and 23nm respectively and the mixed metal oxide $CeBa_{0.5}Fe_{0.5}O_{3-\delta}$ (CBFO-2) with 0.5 mole ratio showed 22nm. Therefore, the average crystallite size increases on substitution compared to pure oxides.

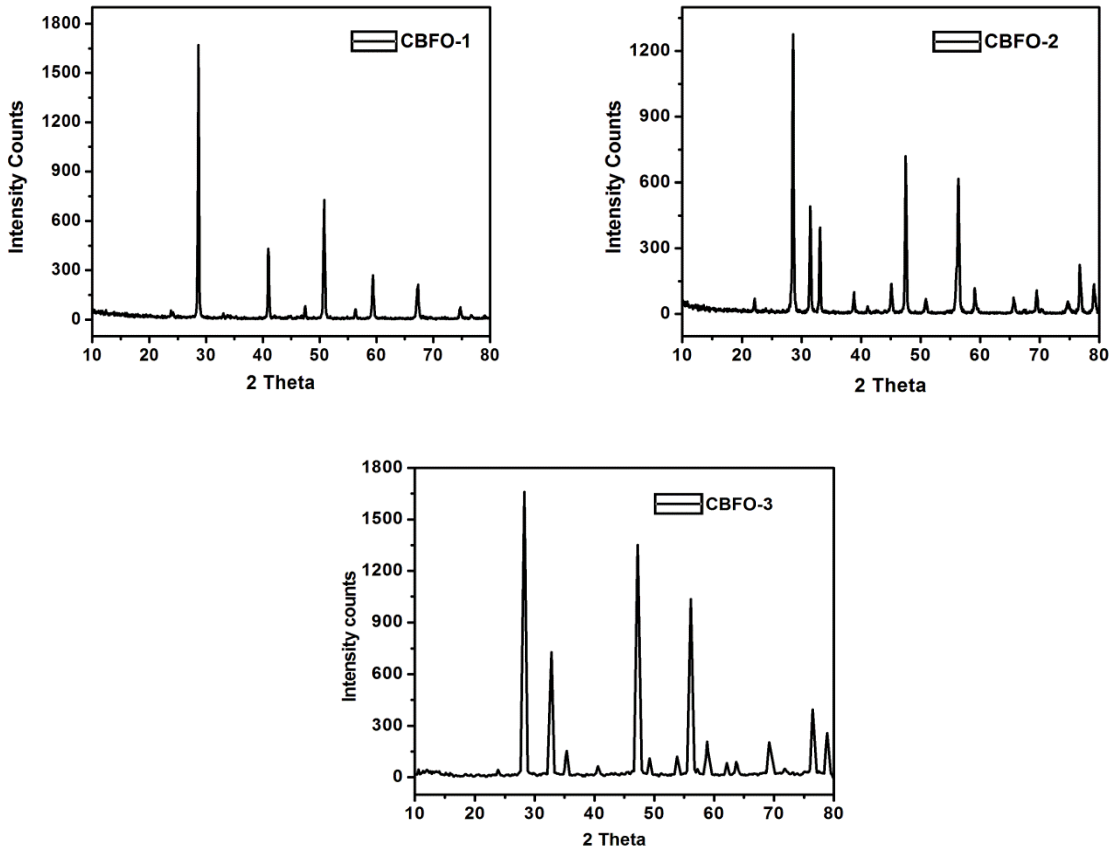

Figure.2. PXRD spectra of CBFO-1, CBFO-2 and CBFO-3 nanoparticl

FT-IR Analysis

FT-IR spectrum helps in determining the appropriate metal-oxide vibrating frequencies and functional groups present in the synthesized materials. Usually, perovskite oxide metal-oxygen frequencies range from 400-1000 cm^{-1}.The pure $CeBaO_3$ (CBFO-1) and $CeFeO_3$ (CBFO-3) oxides exhibited absorption frequencies at 858 and 467; 538 and 480 cm^{-1} respectively. The spectral vibrations at 626 and 534 cm^{-1}confirmed the presence of characteristic metal- oxygen bond in $CeBa_{0.5}Fe_{0.5}O_{3-\delta}$ (CBFO-2) mixed metal oxide as shown in Figure.3.The peaks around 3400 $cm^{-1}$and 1600cm^{-1} correspond to

surface adsorption of water and absorption as a result of the compactions of powder specimen with KBr[27]. This characteristic feature is well-understood in CBFO-2 than in pure mixed metal oxides

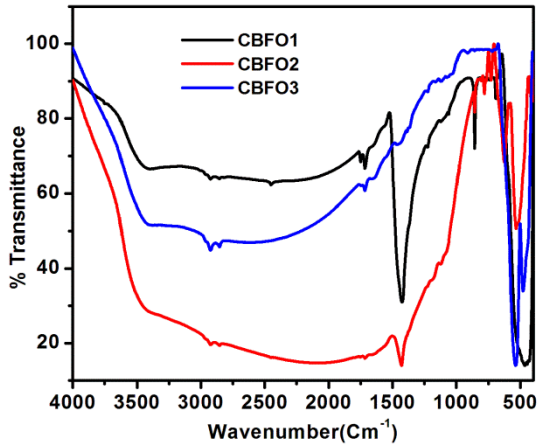

Figure.3 FT-IR spectra of CBFO-1, CBFO-2 and CBFO-3 nanoparticles

Morphological studies

The size, distribution and crystallinity of the synthesized nanoparticles were examined using Transmission Electron Microscope. HRTEM micrographs and SAED patterns of the pure $CeBaO_3$ (CBFO-1) and $CeFeO_3$ (CBFO-3) oxides and $CeBa_{0.5}Fe_{0.5}O_{3-\delta}$ (CBFO-2) mixed metal oxide are represented in Figure.4, Figure.5 and Figure.6 respectively. TEM micrographs indicated that the particles were highly agglomerated in pure $CeFeO_3$ (CBFO-3) oxide and $CeBa_{0.5}Fe_{0.5}O_{3-\delta}$ (CBFO-2) mixed metal oxide due to magnetic characteristic of ferrites [28].The particles are having network like morphology. The brighter spots attained from the selected area electron diffraction (SAED) pattern indicates that the synthesized materials are nanocrystaline in nature. The ring like pattern obtained in SAED confirmed the nano dimension scale of the synthesized oxide materials.

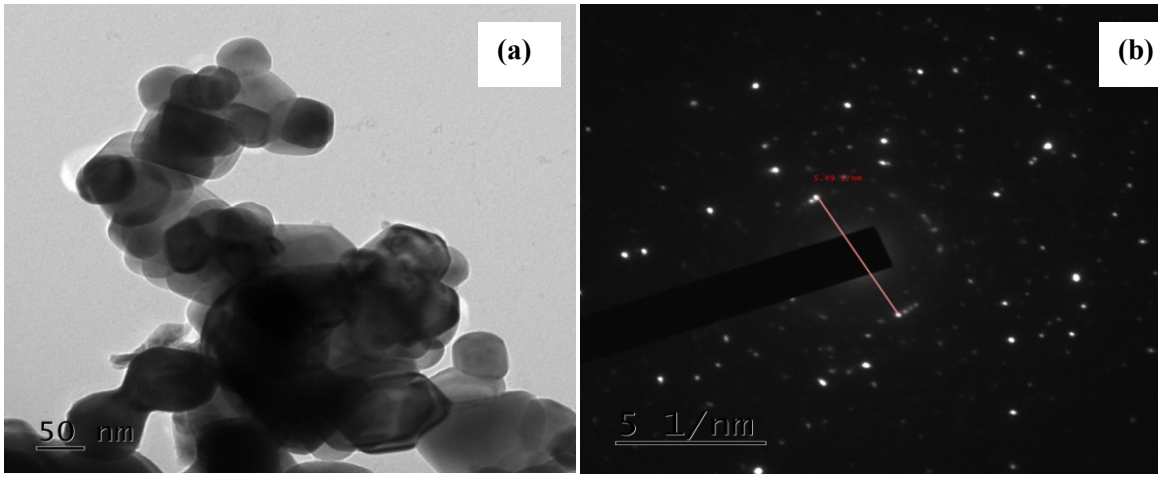

Figure.4.TEM and SAED pattern for CBFO-1 nanoparticles

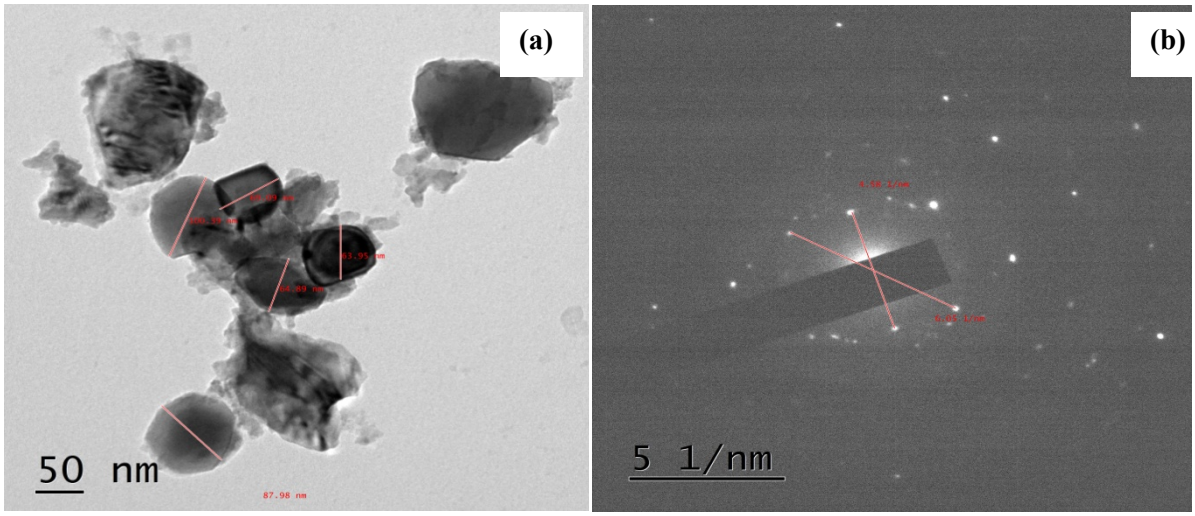

Figure.5.TEM and SAED pattern for CBFO-2 nanoparticles

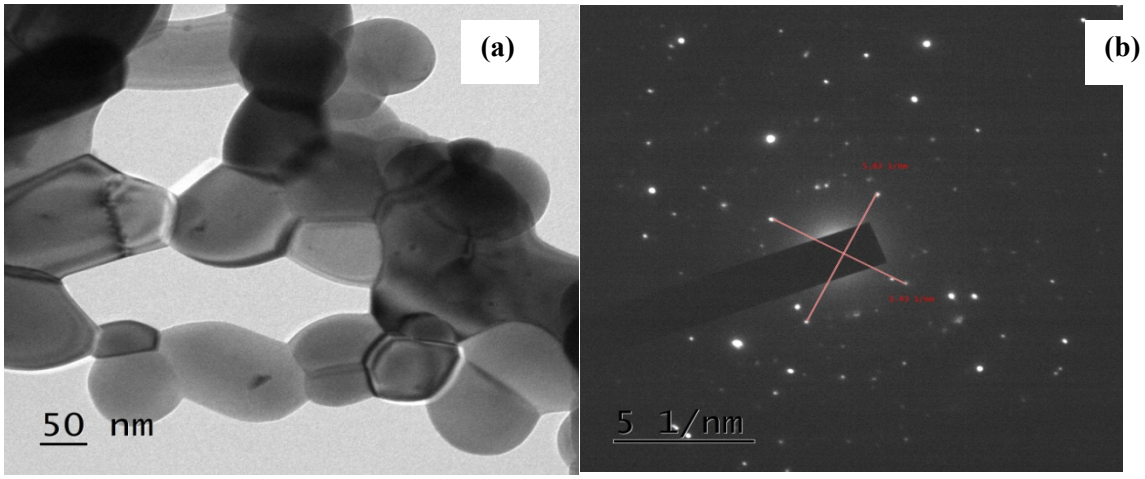

Figure.6. TEM and SAED pattern for CBFO-3 nanoparticles

Optical Properties

UV-Vis absorption spectra of pure and mixed metal oxide nanoparticles are shown in Figure.7. The absorption edge for pure $CeBaO_3$ (CBFO-1) and $CeFeO_3$ (CBFO-3) oxides were found to be 446 and 558nm respectively and 474nm for $CeBa_{0.5}Fe_{0.5}O_{3-\delta}$ (CBFO-2) mixed metal oxide illustrating its suitability for visible light photocatalysis. Therefore, it is observed from the graph that the oxide shifts the absorption edge value to a higher wavelength indicating red shift. According to Ref. [26], nano perovskite which are found to have similar crystal structure through X-ray diffraction studies showed very close values of absorption edges.

The absorption coefficient and band-gap energy is given by the relation as follows: $(F(R)E)^{1/2}=A(E- E_g)$[28] in which E, $E_g$and Aare photon energy, band gap energy and characteristic constant for semiconductors respectively. The band-gap energy was obtained from Kubelka-Munk function verses energy of excited light were 3.22eV, 3.27eV and 2.75eV for $CeBaO_3$ (CBFO-1), $CeBa_{0.5}Fe_{0.5}O_{3-\delta}$ (CBFO-2) and $CeFeO_3$ (CBFO-3) oxides respectively (Figure.8). Therefore, the results indicated that inclusion of divalent alkaline earth cations aids in further increase in band gap energy compared to pure oxides. Minor differences in the band gap energy values were observed from the

Kubelka-Munk plot between the pure and mixed metal oxide nanoparticles. This observation can be related to small variations in crystallite size and created oxygen vacancies in the electronic band structures. The highest value of band gap was observed for $CeBa_{0.5}Fe_{0.5}O_{3-\delta}$ (CBFO-2) mixed metal oxide due to the increased amount of Fe^{2+} as compared to pure $CeFeO_3$(CBFO-3) oxide. Factors such as crystallite size, presence of impurities and structural parameters influence the band gap energy.

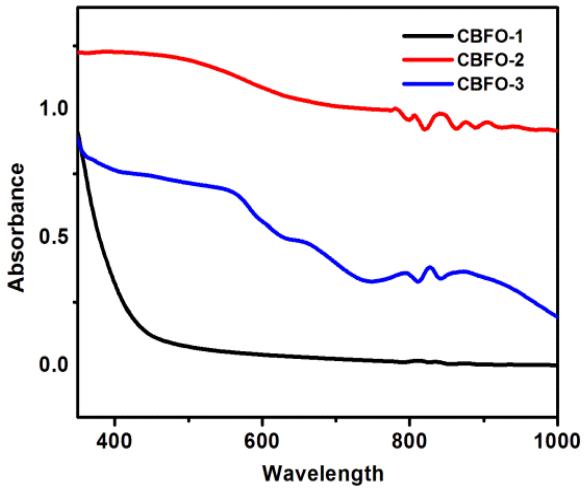

Figure.7.UV- Absorbance spectra of CBFO-1, CBFO-2 and CBFO-3 nanoparticles

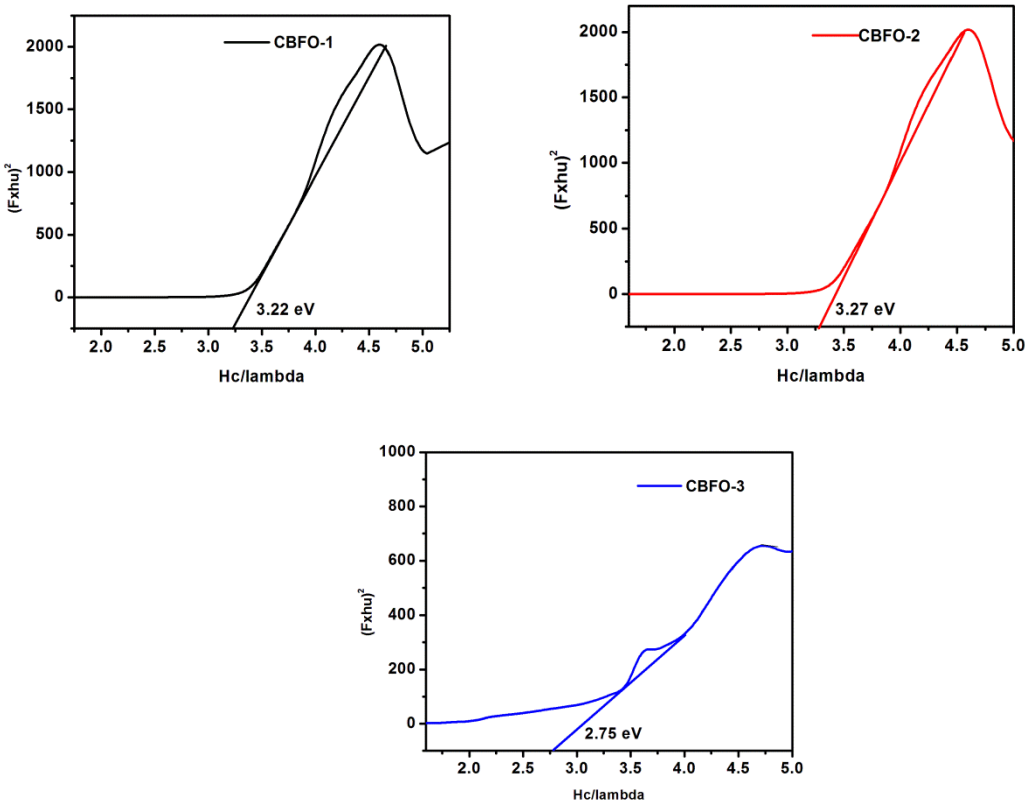

Figure.8. Kubelka-Munk plots of CBFO-1, CBFO-2 and CBFO-3 nanoparticles

Magnetic properties

The magnetic properties of $CeBaO_3$ (CBFO-1), $CeBa_{0.5}Fe_{0.5}O_{3-\delta}$ (CBFO-2) and $CeFeO_3$ (CBFO-3) nanomaterials sintered at 800°C were investigated as shown in Figure.9. When an external magnetic field is applied at room temperature, spontaneous magnetization and hysteresis loops for the synthesized nanomaterials were observed. Formation of magnetic hysteresis loop occurs when a magnetization curve of a ferromagnetic or ferrimagnetic material follows a different demagnetization path. Therefore, the appearance of narrow hysteresis loops indicates weak ferromagnetism[29].The hysteresis loops of mixed metal oxide $CeBa_{0.5}Fe_{0.5}O_{3-\delta}$ (CBFO-2)nanoparticles exhibited weak ferromagnetic behaviour whereas the hysteresis loops of pure $CeBaO_3$ (CBFO-1) and $CeFeO_3$ (CBFO-3) oxides showed ferromagnetic behaviour at room temperature. The magnetic parameters such as saturation magnetization M_s, coercivity H_c, retentivity M_r and squarneness ratio are represented in Table.1

From the VSM graph and values listed in Table.1, it is clear that coercivity of pure $CeFeO_3$ (CBFO-3) oxide is very high as compared to $CeBa_{0.5}Fe_{0.5}O_{3-\delta}$ (CBFO-2) mixed metal oxide, which is a typical behavior of hard ferrites. Therefore it can be concluded that $CeBa_{0.5}Fe_{0.5}O_{3-\delta}$ (CBFO-2) mixed metal oxide is a soft ferrite while $CeFeO_3$ (CBFO-3) comes under the group of hard ferrites. The squareness value of the hysteresis loops were calculated by the ratio of retentivity and magnetization and it was found to be 0.3208 (e.m.u/g), 0.1278 (e.m.u/g), and 0.4223 (e.m.u/g) for CBFO-1, CBFO-2 and CBFO-3 nanoparticles respectively. The magnetic moment is calculated by using the following relation [30]:

$$\mu_{(B)} = M \times M_s/5855 \quad \textbf{(3)}$$

Where M is the molar mass and M_s is the saturation magnetization. The magnetic moment was found to be 0.011; 0.007 for pure oxides ($CeBaO_3$ and $CeFeO_3$) and 0.025 for mixed metal oxide ($CeBa_{0.5}Fe_{0.5}O_{3-\delta}$).

Table.1 VSM measurements of the synthesized nanomaterials

S.No	Sample Code	Coercivity (H_{ci}) (G)	Retentivity (M_r) (e.m.u)	Magnetization (M_s) (e.m.u)	Squareness ratio (e.m.u/g)
1.	$CeBaO_3$	368	25.92E-6	80.79E-6	0.3208
2.	$CeBa_{0.5}Fe_{0.5}O_{3-\delta}$	961	1.07E-3	8.37 E-3	0.1278
3.	$CeFeO_3$	3645	1.66 E-3	3.93 E-3	0.4223

Investigation of Photocatalytic activity of $CeBa_{1-x}Fe_xO_{3-\delta}$ (where x= 0, 0.5 and 1) perovskite oxides

Photo-Fenton activity determines the rate of decolourization of methylene blue dye solution in the presence of catalyst under UV-lamp irradiation. The major absorption band of methylene blue dye at 664 nm in the visible region appeared due to conjugation between two dimethylamine substituted rings through N and S.

The photocatalytic experiments were carried out by addition of 100mg $CeBaO_{3-\delta}$(CBFO-1), $CeBa_{0.5}Fe_{0.5}O_{3-\delta}$(CBFO-2)and $CeFeO_3$ (CBFO-3) catalysts to 25ppm of 100mL methylene blue dye solution in quartz tubes. Before illumination, the adsorption-desorption equilibrium between the photocatalysts and methylene blue dye solution was studied by stirring in dark for about 30 minutes. During the dark reaction, 5.06% decolourization was observed for $CeBa_{0.5}Fe_{0.5}O_{3-\delta}$(CBFO-2)mixed metal oxide nanoparticles whereas 0.67% and 1.35% decolourization was observed for $CeBaO_3$(CBFO-1) and $CeFeO_3$ (CBFO-3) pure oxides. No reactivity in methylene blue dye solution was observed both in

presence and absence of UV-lamp irradiation. No significant degradation with time was observed in the presence of dye and photocatalysts without the addition of hydrogen peroxide.

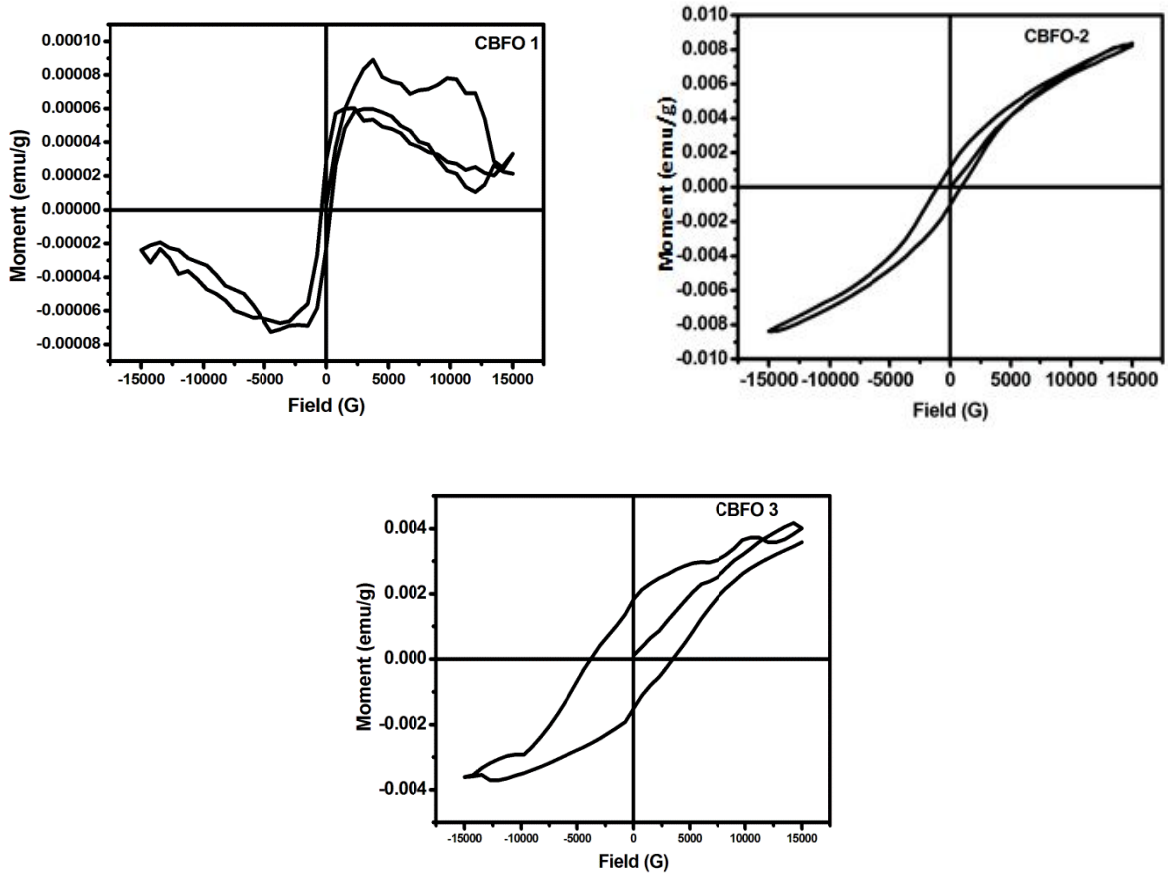

Figure.9.VSM of CBFO-1, CBFO-2 and CBFO-3 nanoparticles

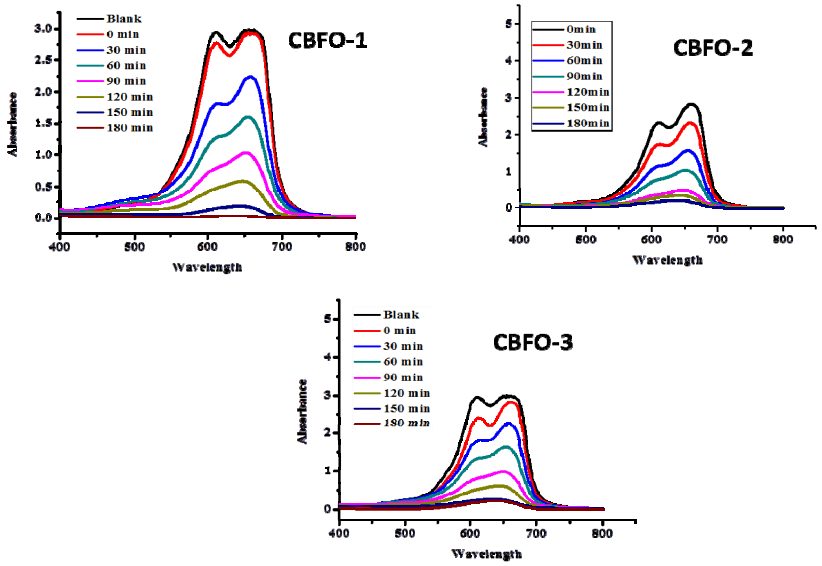

Figure.10.Absorption spectra in the presence of CBFO-1, CBFO-2 and CBFO-3 nanoparticles as photocatalysts

Therefore, preliminary results concluded that presence of oxygen, catalyst and UV-lamp irradiation was required for dye decolourization studies. The degradation of methylene blue dye under visible-light illumination was known as an effective method to evaluate photocatalytic activity of the orthoferrite nanoparticles. It is clearly understood from the graph that with increasing reaction time, reduction in absorption bands of the methylene blue dye was observed. Figure.10 shows the reduction in absorption spectra with time for CBFO-1, CBFO-2 and CBFO-3 nanoparticles respectively. Higher decolourization efficiency of 99.28% was achieved for $CeBa_{0.5}Fe_{0.5}O_{3-\delta}$(CBFO-2) nanoparticles when compared to pure oxides. The strong absorption bands in the visible-light region [25] are due to the higher oxygen vacancies $CeBa_{0.5}Fe_{0.5}O_{3-\delta}$ mixed metal oxide (δ=1.12) (Figure.11) as compared to $CeBaO_3$ and $CeFeO_3$pure oxides.

Based on the above results obtained, the possible mechanism proposed for photodegradation of Methylene Blue dye (MB) on $CeBa_{1-x}Fe_xO_{3-\delta}$(x=0, 0.5 and 1) nano perovskite oxide is as follows [28]:

$$CeBa_{1-x}Fe_xO_{3-\delta} \xrightarrow{h\nu} CeBa_{1-x}Fe_xO_{3-\delta}[h^+(VB) + e^-(CB)] \quad \textbf{(4)}$$

$$Fe^{3+} + H_2O_2 \longrightarrow Fe^{2+} + {\bullet}OOH + H^+ \quad \textbf{(5)}$$

$$Fe^{3+} + {\bullet}OOH + H^+ \longrightarrow Fe^{2+} + O_2 + 2H^+ \quad \textbf{(6)}$$

$$Fe^{2+} + H_2O_2 \longrightarrow Fe^{3+} + OH^- + {\bullet}OH \quad \textbf{(7)}$$

$$MB + h\nu \longrightarrow MB^* \quad \textbf{(8)}$$

$$MB^* + CeBa_{1-x}Fe_xO_{3-\delta}(VB) \longrightarrow CeBa_{1-x}Fe_xO_{3-\delta} + MB^+ \quad \textbf{(9)}$$

$$MB \text{ (or } MB^+) + {\bullet}OH \longrightarrow \text{Degraded products} \quad \textbf{(10)}$$

Therefore, for mixed metal oxide /hydrogen peroxide system, the simultaneous presence of $CeBa_{0.5}Fe_{0.5}O_{3-\delta}$nanoparticles and H_2O_2 markedly enhanced the Photodecolourization of methylene blue dye, which implies that $CeBa_{0.5}Fe_{0.5}O_{3-\delta}$ nanoparticles acts as an efficient heterogeneous fenton-like catalyst compared to pure oxides.

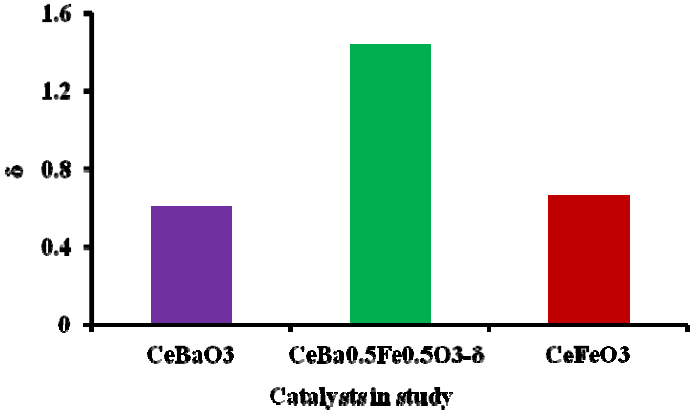

Figure.11.Oxygen non-stoichiometry (δ) verses Catalysts in study

Chemical kinetic studies of synthesized photocatalysts

According to Langmuir Hinshelwood (L-H) model[31, 32]the photocatalytic degradation of methylene blue dye in the presence of $CeBa_{1-x}Fe_xO_{3-\delta}$ (x= 0, 0.5 and 1) followed pseudo first order kinetics.

$$r = -\frac{dc}{dt} = \frac{k_1 KC}{1 + K_{LH}C} = kC \quad \textbf{(11)}$$

where r is rate of reaction in $mgL^{-1}min^{-1}$, k_r is reaction rate constant in $mgL^{-1}min^{-1}$, $K_{LH}$is the adsorption rate constant in Lmg^{-1}, C is concentration of the reactant in mgL^{-1}, t is the time of irradiation in min and k, pseudo first order rate constant in min^{-1}

By integrating in limit of $C=C_o$at t=0, the above equation can be expressed as $$\ln\frac{Co}{C} = kt \qquad \textbf{(12)}$$

The linear plot of $-\ln (C/C_o)$ Vs time for all the catalysts CBFO-1, CBFO-2 and CBFO-3 are shown in Fig.12

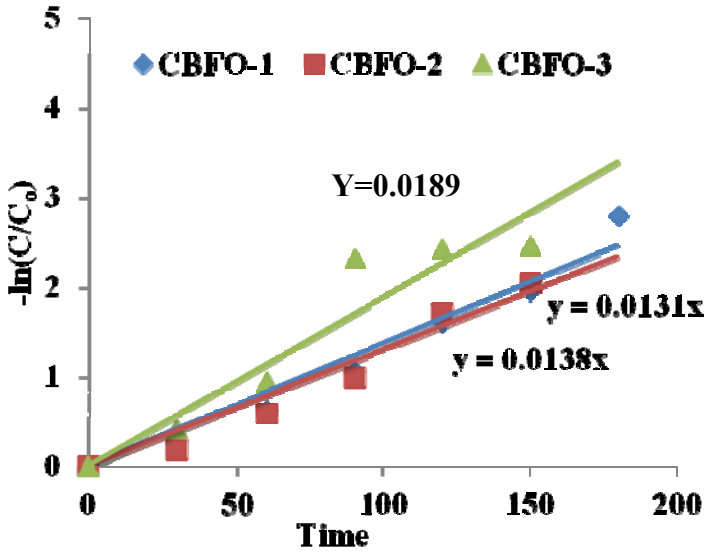

Figure.12 Photo-degradation kinetics of CBFO-1, CBFO-2 and CBFO-3 nanoparticles

Degradation efficiency of the synthesized photocatalysts

The catalytic activity of $CeBa_{0.5}Fe_{0.5}O_{3-\delta}$ (CBFO-2) mixed metal oxide nanoparticles was much higher than those of pure oxides ($CeBaO_3$ and $CeFeO_3$) as represented in Figure.13. The higher efficiency of $CeBa_{0.5}Fe_{0.5}O_{3-\delta}$ mixed metal oxide may be due to higher oxygen vacancies as compared to pure oxides. The magnetic and visible-light property of $CeFeO_3$ pure oxide also makes it act as a photocatalyst.

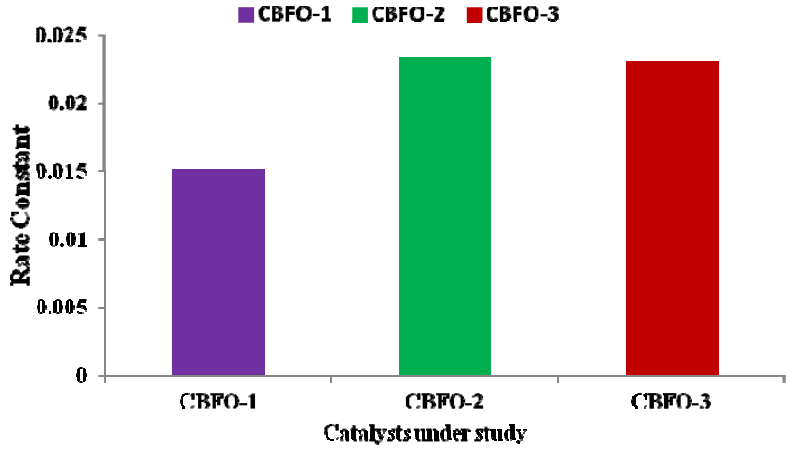

Figure.13 Degradation efficiency of CBFO-1, CBFO-2 and CBFO-3 photocatalysts

Conclusion

In summary, $CeBa_{1-x}Fe_xO_{3-\delta}$ nano perovskites with varying mole ratios (X=0, 0.5 and 1), prepared via citric acid sol-gel process was characterized and studied for degradation of methylene blue dye under UV and visible light irradiation. The average crystallite size obtained from XRD ranges between 22-36nm which revealed the synthesized materials are nanocrystalline in nature. The IR bands at 626 and 534 cm^{-1}confirmed the presence of characteristic metal- oxygen bond in $CeBa_{0.5}Fe_{0.5}O_{3-\delta}$(CBFO-2) mixed metal oxide. The band-gap energy values of 3.22eV, 3.27eV and 2.75eV obtained from Kubelka-Munk plots for $CeBaO_3$ (CBFO-1), $CeBa_{0.5}Fe_{0.5}O_{3-\delta}$(CBFO-2) and $CeFeO_3$ (CBFO-3) oxides indicated that the presence of divalent alkaline earth cations aids in further increase in band gap energy compared to pure oxides. The magnetic measurements obtained from VSM analysis showed that $CeBa_{0.5}Fe_{0.5}O_{3-\delta}$ mixed metal oxide nanoparticles were weakly ferromagnetic as compared to pure oxides which were ferromagnetic. Among the synthesized catalysts, it was notable that nano perovskite $CeBa_{0.5}Fe_{0.5}O_{3-\delta}$ (CBFO-2) mixed metal oxide nanoparticles could degrade the methylene blue azo dye and act as photo-fenton like photocatalyst more efficiently when compared to other similarly existing pure oxide photocatalysts.

References

[1] Kanta, Dheeraj Kumar, Study the perovskite- type mixed metal oxides with the general formula ABO3, IJRST,3, 1-5, 2014.

[2] W Zi-Xian, W Yan, L Ji-Ping, X Cai-Mei, Z Wei-Wei, Synthesis, magnetization and photocatalytic activity of LaFeO3 and $LaFe_{0.5}Mn_{0.5}$-$xO_{3-\delta}$, Mater. Chem. Phys., 136,755-761, 2012.

[3] HY Hwang. Perovskites: Oxygen vacancies shine blue. Nat. Mater., 4,803-804, 2005.

[4] LA Han, CL Chen, HY Dong, JY Wang, GM Gao, Physica B., 403,2614-2617,2008.

[5] J Saeid, A Majid, G Hamid, A Asiyeh, KA Amirsalar,Study on the synthesis and magnetic properties of the cerium ferrite ceramic,J Alloys Compd., 694,800-807,2017.

[6] TS Zhang, J Ma,LB Kong, SH Chan, JA Kilner, Aging behavior and ionicconductivity of ceria-based ceramics: a comparative study. Solid State Ion.,170, 209-217, 2004.

[7] G Michael, Dye-sensitized solar cells,J. Photochem. Photobiol. C: Photochem. Rev., 4, 145-153, 2003.

[8] J Ameta, A Kumar, R Ameta, VK Sharma, SC Ameta, Synthesis and characterization of $CeFeO_3$ photocatalyst used in photocatalytic bleaching ofgentian violet, J. Iran. Chem. Soc. 6, 293-299, 2009.

[9] A Wu, H Shen, JXu, Z Wang, L Jiang, L Luo, S Yuan, S Cao, H Zhang, Crystalgrowth and magnetic property of $YFeO_3$ crystal, Bull. Mater. Sci.35,259-263, 2012.

[10] A Abbad, W Benstaali, HA Bentounes, S Bentata, Y Benmalem, Search for half-metallic ferromagnetism in orthorhombic Ce(Fe/Cr)O_3 perovskites, Solid State Commun., 228,36-42,2016.

[11] JL Ye, CC Wang, W Ni, XH Sun. Dielectric properties of $ErFeO_3$ ceramics over a broad temperature range, J. Alloys Compd.,617,850-854, 2014.

[12] C Chen, KB Xu, CC Wang, YM Cui, Polaronic relaxation in $LaFeO_3$, Mater.Lett., 89,153-155,2012.

[13] J Wang, DN Tafen, JP Lewis, Z Hong, A Manivannan, M Zhi, M Li, N Wu. Origin of photocatalytic activity of nitrogen-doped TiO_2nanobelts. J. Am. Chem. Soc., 131, 12290-12297, 2009.

[14] Y Cong, J Zhang, F Chen, M Anpo, D He. Preparation, photocatalytic activity and mechanism of nano-TiO_2 co-doped with nitrogen and iron (III), J. Phys.Chem., 111,10618-10623, 2007.

[15] L Kumaresan, M Mahalakshmi, M Palanichamy, V Murugesan, Synthesis,characterization, and photocatalytic activity of Sr doped TiO_2nanoplates, Ind. Eng. Chem. Res.,49, 1480-1485, 2010.
[16] J Papp, S Soled, K Dwight, A Wold. Surface acidity and photocatalytic activityof TiO_2, WO_3/TiO_2, and MoO_3/TiO_2 photocatalysts. Chem. Mater.,6,496-500, 1994.
[17] TH Shin, SIda, TIshihara, Doped CeO_2-$LaFeO_3$ composite oxide as an activeanode for direct hydrocarbon-type solid oxide fuel cells. J. Am. Chem. Soc., 133, 19399-19407, 2011.
[18] H Aono, MTomida, YSadaoka, Conventional synthesis method for fine polymetallic $LaFeO_3$ using ethylene glycol solvent addition, J. Ceram. Soc. Jpn, 117, 1048-1051, 2009.
[19] PVGosavi, RBBiniwale, Pure phase $LaFeO_3$ perovskite with improved surface area synthesized using different routes and its characterization, Mater. Chem. Phys., 119,324-329, 2010.
[20] L Ju, ZChen, LFang, WDong, FZheng, MShen, Sol-gel synthesis andphoto-fenton- like catalytic activity of $EuFeO_3$ nanoparticles, J. Am. Ceram. Soc., 94, 3418-3424, 2011.
[21] H Takuya, T Shingo, I Fumihiro, O Ayako, N Atsuko, Y Yuh, M Akiyuki, Y Jinhua, Photocatalytic activities of Ba_2RBiO_6 (R= La, Ce, Nd, Sm, Eu, Gd, Dy) under visible light irradiation. J. Ceram. Soc. Jpn, 118, 91-95, 2010.
[22] Sun M, Jiang Y, Li F, Xia M, Xue B, Liu D. Dye Degradation Activity and Stability of Perovskite-Type $LaCoO_{3-x}$ (x=~0.075), Mater Trans.,51,2208-2214, 2010.
[23] D Wang, Z Zou, J Ye, A new spinel-type photocatalyst $BaCr_2O_4$ for H_2 evolution underUV and visible light irradiation, Chem. Phy. Lett.,373,191-196,2003.
[24] M Shao, J Han, M Wei, DG Evans, X Duan. The synthesis of hierarchicalZn-Ti layered double hydroxide for efficient visible-light photocatalysis, Chem. Eng. J.,168, 519-524, 2011.
[25] P Pasierb, J Wyrwa, M Rekas. Electrical Properties of Acceptor-Doped $BaCeO_3$.Ceram Mater., 62,311-315, 2010.
[26] M Bradha, T Vijayarhavan, SP Suriyaraj, Selvakumar, MA Anuradha. Synthesis of photocatalytic $La_{(1-x)}A_xTiO_{3.5-\delta}$ (A= Ba, Sr, Ca) nano perovskites and their application for photocatalytic oxidation of congo red dye in aqueous solution, J Rare Earths., 33,160167,2015.
[27] B Avila Josephine, A Manikandan, V Mary Teresita, S Arul Antony, Fundamental study of $LaMg_xCr_{1-x}O_{3-\delta}$ perovskites nano-photocatalysts: Sol-gel synthesis, characterization and humidity sensing, Korean J. Chem. Eng.,33,1590-1598,2016.
[28] L Li, Z Min, T Peng, G Wen, W Xiong. Synergistic photocatalytic activity of $LnFeO_3$ (Ln=Pr, Y) perovskites under visible-light illumination. Ceram Int.40, 13813-13817, 2014.
[29] MA Gabal, RS Al-luhaibi, YMAlAngar,Mn–Zn nano-crystalline ferrites synthesized from spent Zn–C batteries using novel gelatin method. J. Hazard. Mater.,246,227-233, 2013.
[30] P Annie Vinosha, Belina Xavier, A Ashwini, AnselMely L, Jerome Das S.Tailoring the photo-Fenton activity of Nickel ferrite nanoparticles synthesized by low temperature coprecipitation technique,Optik.,137,244-253, 2017.
[31] T Soltani and MH Entezari, Photolysis and photocatalysis of methylene blue by ferrite bismuth nanoparticles under sunlight irradiation. J. Mol. Catal. A-Chem., 377, 197-203, 2013.
[32] T Soltani and MH Entezari, Solar photocatalytic degradation of RB5 by ferrite bismuth nanoparticles synthesized via ultrasound. Ultrason Sonochem, 20, 1245-1253, 2013.